

# Precision half-life measurement of the $\beta^+$ decay of $^{37}\text{K}$

P.D. Shidling<sup>1,\*</sup>, D. Melconian<sup>1,2</sup>, S. Behling<sup>1,3</sup>, B. Fenker<sup>1,2</sup>, J.C. Hardy<sup>1,2</sup>, V.E. Iacob<sup>1</sup>,  
E. McCleskey<sup>1,2</sup>, M. McCleskey<sup>1,2</sup>, M. Mehlman<sup>1,2</sup>, H.I. Park<sup>1,2</sup> and B.T. Roeder<sup>1</sup>

<sup>1</sup> Cyclotron Institute, Texas A&M University, College Station, Texas, 77843-3366

<sup>2</sup> Department of Physics, Texas A&M University, College Station, Texas, 77843-4242

<sup>3</sup> Department of Chemistry, Texas A&M University, College Station, Texas, 77843-302

(Dated: November 16, 2021)

The half-life of  $^{37}\text{K}$  has been measured to be 1.23651(94) s, a value nearly an order of magnitude more precise than the best previously reported. The  $\beta^+$  decay of  $^{37}\text{K}$  occurs mainly via a superallowed branch to the ground-state of its  $T = 1/2$  mirror,  $^{37}\text{Ar}$ . This transition has been used recently, together with similar transitions from four other nuclei, as an alternative test of CVC and method for determining  $V_{ud}$ , but the precision of its  $ft$  value was limited by the relatively large half-life uncertainty. Our result corrects that situation. Another motivation for improving the  $ft$  value was to determine the standard-model prediction for the  $\beta$ -decay correlation parameters, which will be compared to those currently being measured by the TRINAT collaboration at TRIUMF. The new  $ft$  value, 4605(8) s, is now limited in precision by the 97.99(14)% ground-state branching ratio.

PACS numbers: 21.10.Tg, 23.40.-s, 27.30.+t

## I. INTRODUCTION

Many precision measurements of the correlation parameters and  $ft$  values of  $\beta$ -decaying nuclei have been used to help form our understanding of the fundamental symmetries of the weak interaction. Experiments of this kind continue to be performed to search for physics beyond the standard model. For example, the measured  $ft$  values for superallowed  $J^\pi = 0^+ \rightarrow 0^+$  pure Fermi transitions, have been used to verify the conserved vector current (CVC) hypothesis to one part in  $10^4$ ; to determine most precisely the value of  $V_{ud}$ , the up-down element of the Cabbibo-Kobayashi-Maskawa (CKM) matrix; and to set limits on scalar and right-handed currents [1–3].

Transitions between isospin  $T = 1/2$  doublets in mirror nuclei are also useful weak-interaction probes because there are relatively few corrections required to describe their decay. The most thoroughly studied and theoretically cleanest example of such a transition is the decay of the neutron [4–6], but a number of other cases have attracted attention recently: the decays of  $^{19}\text{Ne}$ ,  $^{21}\text{Na}$ ,  $^{29}\text{P}$ ,  $^{35}\text{Ar}$  and the subject of the present work,  $^{37}\text{K}$ . Naviliat-Cuncic and Severijns [7] used the  $ft$  values for these five transitions to determine  $V_{ud}$ , though less precisely than has been achieved from the  $0^+ \rightarrow 0^+$  transitions. With more precise measurements, however, the  $T = 1/2$  result for  $V_{ud}$  could be improved enough to provide a valuable cross-check on the result from the  $0^+ \rightarrow 0^+$  transitions. Our measurement is a first step on this path.

For mixed Fermi/Gamow-Teller transitions, such as the decay of  $^{37}\text{K}$  to the ground state of  $^{37}\text{Ar}$ , the measured  $ft$  value can be related to  $V_{ud}$  via the corrected  $\mathcal{F}t$  value, which incorporates calculated corrections for radiative and isospin-symmetry-breaking effects, as fol-

lows [8]:

$$\mathcal{F}t = \frac{f_V t (1 + \delta'_R) (1 + \delta_{\text{NS}}^V - \delta_C^V)}{K} = \frac{f_V t (1 + \delta'_R) (1 + \delta_{\text{NS}}^V - \delta_C^V)}{G_F^2 |V_{ud}|^2 C_V^2 |M_F^0|^2 (1 + \Delta_R^V) \left[ 1 + \left( \frac{f_A}{f_V} \right) \rho^2 \right]} \quad (1)$$

where  $K/(\hbar c)^6 = 2\pi^3 \ln 2 \hbar / (m_e c^2)^5 = 8120.278(4) \times 10^{-10} \text{ GeV}^{-4}\text{s}$ , the Fermi constant  $G_F/(\hbar c)^3 = 1.16637(1) \times 10^{-5} \text{ GeV}^{-2}$ , and the vector coupling constant  $C_V = 1$ . The parameters  $\delta'_R$ ,  $\delta_C^V$ ,  $\delta_{\text{NS}}^V$  and  $\Delta_R^V$  are the usual radiative and isospin-symmetry-breaking correction terms calculated for the vector current [3]. The statistical rate functions for vector and axial-vector currents are denoted  $f_V$  and  $f_A$ . In these mirror nuclei their ratio  $f_A/f_V$  generally is within a few percent of unity according to shell model calculations [8].

The Fermi matrix element in the limit of strict isospin-symmetry is

$$M_F^0 = [T(T+1) - T_Z(T_Z \pm 1)]^{1/2} \quad (2)$$

for a  $\beta^\pm$  transition from a nucleus having  $Z$  protons,  $N$  neutrons, and isospin  $T_Z = \frac{1}{2}(N - Z)$ . It takes the value 1 for  $T=1/2$  mirror transitions.

Finally, the Gamow-Teller to Fermi mixing ratio  $\rho$  is given by

$$\rho = \frac{C_A M_{GT}^0}{C_V M_F^0} \left[ \frac{(1 + \delta_{\text{NS}}^A - \delta_C^A)(1 + \Delta_R^A)}{(1 + \delta_{\text{NS}}^V - \delta_C^V)(1 + \Delta_R^V)} \right]^{1/2}, \quad (3)$$

where  $M_{GT}^0$  is the Gamow-Teller matrix element,  $C_A$  is the axial-vector coupling constant, and the correction terms with  $A$  superscripts are equivalent to those with  $V$  superscripts but must be evaluated for the axial-vector component. Since, in general,  $C_A M_{GT}^0$  cannot be precisely calculated,  $\rho$  must be taken from experiment. This also makes it unnecessary to calculate the axial-vector correction terms.

\* pshidling@comp.tamu.edu

The decay of  $^{37}\text{K}$  was one of the five cases used in Ref. [7] to determine  $V_{ud}$ . The relatively large uncertainty of its contribution was overwhelmingly dominated by the precision of  $\rho$ , which was obtained from a single  $\pm 3\%$  measurement of the neutrino asymmetry parameter,  $B_\nu$  [9]. The  $\mathcal{F}t$  value is known much better, to  $\pm 0.6\%$  [8], with the largest contribution to its uncertainty being the lifetime of the decay. A survey of mirror transitions and the theoretical corrections to their  $f_V t$  values was made in Ref. [8], in which three  $^{37}\text{K}$  half-life measurements [10–12] were averaged to arrive at  $t_{1/2} = 1.2248(73)$  s. This  $\pm 0.60\%$  uncertainty is much larger than the  $\pm 0.14\%$  and  $\pm 0.04\%$  uncertainties on the other two contributors to  $f_V t$  for  $^{37}\text{K}$ : the branching ratio and  $f_V$  value, respectively.

The aim of the present work is to improve the lifetime of  $^{37}\text{K}$  so that it no longer dominates the uncertainty in the deduced  $\mathcal{F}t$  value. A more precise  $\mathcal{F}t$  value on its own will not improve the value of  $V_{ud}$  obtained from  $^{37}\text{K}$  decay. For that purpose, an improved measurement of  $\rho$  via a correlation parameter such as  $B_\nu$  or  $A_\beta$  is necessary.

## II. EXPERIMENT

A high purity radioactive beam is essential for performing a precision half-life measurement. We have measured the half-life of  $^{37}\text{K}$  at the Cyclotron Institute of Texas A&M University using a  $4\pi$  continuous-gas-flow proportional counter and a fast tape-transport system. We produced  $^{37}\text{K}$  via an inverse kinematics reaction (fusion-evaporation reaction) by accelerating a primary beam of  $^{38}\text{Ar}$  to 29 MeV/u in the K500 superconducting cyclotron, and impinging it on a 1.6-atm  $\text{H}_2$  gas target cooled to liquid nitrogen temperature. The forward focused reaction products were analyzed using the Momentum Achromat Recoil Separator (MARS) [13, 14]. Selection and focusing of the desired ions in MARS was done according to their  $m/q$  value. At the focal plane of MARS, a 16-strip position-sensitive detector of 300  $\mu\text{m}$  thickness with an active area of  $5 \times 5$   $\text{cm}^2$  could be inserted to detect the secondary reaction products, which were identified according to their position and energy loss in the strip detector. The position of the reaction products on the strip detector was related with its  $m/q$  ratio. This detector was initially inserted to help us tune the spectrometer and was then removed before the measurement began. During the measurement, it was reinserted once a day to ensure that no changes had occurred. In this way we determined that the 22.7-MeV/u  $^{37}\text{K}$  beam passing through the spectrometer extraction slits was 98.4% pure, the remaining contaminants being  $^{35}\text{Ar}$ ,  $^{34}\text{Cl}$  and  $^{33}\text{Cl}$ .

This separated beam then exited the vacuum system through a 51  $\mu\text{m}$  thick Kapton foil. Immediately following this foil was a 0.3 mm-thick BC-404 plastic scintillator, which counted the number of ions. The beam then passed through a stack of Al degraders, and finally was

implanted into the 76- $\mu\text{m}$ -thick aluminized Mylar of the fast-tape transport system. The degrader thickness was adjusted so as to place the implanted  $^{37}\text{K}$  at a depth mid-way through the tape. At this setting (51  $\mu\text{m}$  of Al), the combination of electromagnetic separation in MARS and range selection in the degraders resulted in the  $^{37}\text{K}$  beam reaching the tape being  $> 98.8\%$  pure.

For part of the measurement we used two different thicknesses of degrader: 70  $\mu\text{m}$ , which resulted in the  $^{37}\text{K}$  being placed at the front of the tape; and 13  $\mu\text{m}$ , which put it at the back of the tape. The former led to a higher proportion of impurities; the latter to a much lower proportion. In both cases the intensity of  $^{37}\text{K}$  was reduced. In the best case, with the  $^{37}\text{K}$  deposited near the back of the tape, the sample purity was  $> 99.7\%$ .

A sample of  $^{37}\text{K}$  was collected by implanting the beam into a section of aluminized Mylar tape for a time interval of 0.5 s. The beam was then turned off and the tape-transport system moved the sample in 170 ms to a well-shielded location, stopping it in the center of a  $4\pi$  proportional gas counter. There, the  $\beta$  particles from the decay were counted for  $\approx 20$  half-lives (25 s). This cycle was repeated continuously, with each sample being collected on a fresh region of tape, until the desired statistics had been accumulated.

The  $4\pi$  gas counter and the data acquisition system used in the present measurement were similar to those originally described in Ref. [15]. The current system has also been described in detail in reports of previous half-life measurements of superallowed  $\beta^+$  emitters performed at Texas A&M University (see, for example, [16, 17]). Briefly, the preamplified signals from the gas counter are passed to a fast-filter amplifier with a high gain ( $\times 500$ ). At this high gain many of the pulses would saturate the amplifier so, to ensure that the amplifier recovers quickly, large pulses are clipped with a Schottky diode inserted after the first stage of amplification. The amplified and clipped pulses are then sent to a discriminator with very low threshold (150 – 250 mV).

Since deadtime is a serious concern for half-life measurements, the discriminator signals were split and sent to two fixed-width nonretriggering and nonextending gate generators, which established different dominant deadtimes in the two separate streams, both of which were multiscaled into 500-channel time spectra.

The total measurement was split into 13 runs with different experimental conditions: three discriminator threshold settings (150, 200 and 250 mV), two combinations of dominant deadtimes (4 and 6  $\mu\text{s}$ ; 3 and 8  $\mu\text{s}$ ), three detector bias voltages within the detector's plateau region (2600, 2650 and 2700 V) and three degrader thicknesses (13, 51 and 70  $\mu\text{m}$ ). The initial activity of  $^{37}\text{K}$  for each cycle was in the range of 4000 – 7000 cps. All runs were composed of 100 – 300 cycles, which yielded a total of  $4 \times 10^6$  counts in each. In addition, a background measurement was performed for which all conditions were the same as for normal data taking except that the tape motion was disabled. The background rate was found to be

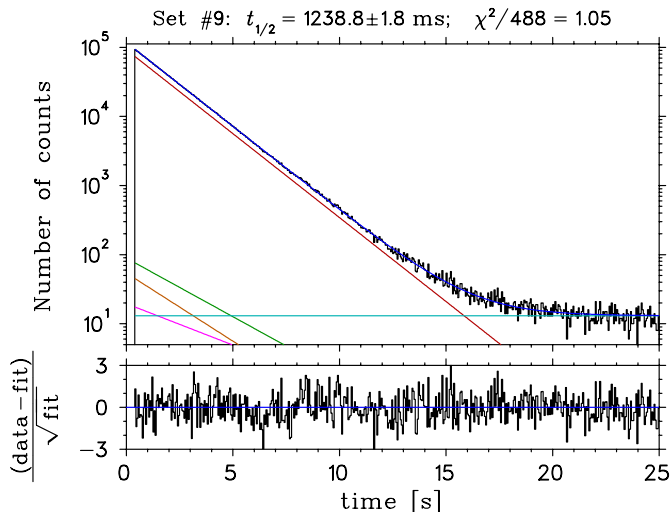


FIG. 1. (Color online) Typical summed decay curve of the deadtime-corrected data obtained from a single run (top) and corresponding residuals of the fit (bottom). The  $^{37}\text{K}$  decay curve accounts for 99.5% of the data, with 0.27% from the  $^{35}\text{Ar}$  and  $^{33,34}\text{Cl}$  contaminants, and the rest from background. The reduced  $\chi^2$  of the fit was 1.05 with 488 degrees of freedom.

four orders of magnitude lower than the initial count rate for each collected sample.

### III. DATA ANALYSIS

The selection of data for final analysis was made according to three criteria. First, cycles with too few counts – less than 5000 – were rejected. Second, the number of  $\beta$ 's recorded in each cycle was compared to the corresponding number of heavy ions recorded in the scintillator at the exit of MARS. If their ratio was abnormally low, it meant that the tape did not stop with the activity positioned correctly within the  $4\pi$  proportional gas counter. In that case, the cycle was rejected. Finally, a cycle was rejected if a half-life fit of the recorded data resulted in a very poor reduced  $\chi^2 > 1.3$ , which corresponds to a goodness-of-fit statistic less than 0.001%.

We analyzed the decay data from accepted cycles using two different methods: one based on summing all accepted cycles in a run (“summed” analysis) and the other on performing a simultaneous fit on all the cycles of a run (“global” analysis). All fits employed a fortran code based on the Marquardt algorithm for  $\chi^2$  minimization. The program assumes Poisson rather than Gaussian statistics in the data.

The fit function contained a constant background plus four exponentials corresponding to the decays of  $^{37}\text{K}$  and the main contaminants  $^{35}\text{Ar}$ ,  $^{34}\text{Cl}$  and  $^{33}\text{Cl}$ . The half-lives of the contaminants were fixed at their well-known measured values:  $t_{1/2} = 1.7752(10)$  s for  $^{35}\text{Ar}$  [8],  $1.52655(44)$  s for  $^{34}\text{Cl}$  [3] and  $2.5111(40)$  s for  $^{33}\text{Cl}$  [8]. The intensity of the contaminants could not be fit sepa-

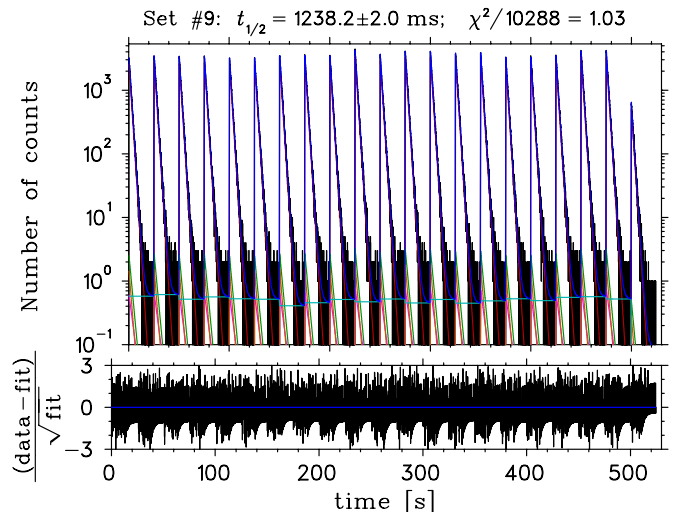


FIG. 2. (Color online) Simultaneous fit to the 21 decay curves of a single run containing a total of 311 cycles combined into groups of 15 (top) and corresponding residual plot (bottom). The data here are the same as shown in Fig. 1 except in this case the data are not summed to a single decay curve. Here the reduced  $\chi^2$  is 1.025 with 6858 degrees of freedom.

rately because of the high correlations between them, so we fixed the relative normalization of the contaminants at the values measured in the MARS focal-plane detector (corrected for losses in the degraders), and allowed only the total amount of contaminant activity to vary relative to  $^{37}\text{K}$  in the fitting procedure.

In the “summed” method of analysis, the first step was to correct the measured decay spectrum in each cycle channel-by-channel for deadtime, based on the measured rate in each channel. Next, the cycles of a given run were summed into two decay curves, one for each imposed dominant deadtime. Finally, these spectra were fitted as already described. Figure 1 shows a typical deadtime-corrected decay curve for a single run analyzed using the summed analysis technique. Note that the fitted background level in the figure agrees well with the value obtained in our dedicated background run.

In the “global” analysis, the fitting function itself is adjusted to account for deadtime effects. In this method, many separate decay spectra within a single run were fit simultaneously, all with the same lifetime for  $^{37}\text{K}$  but with separate contamination levels and backgrounds allowed for each spectrum. Runs had between 120 and 750 cycles; so, to create a more manageable number of spectra and also to improve the statistics in the individual spectra, we summed the cycles together in groups and for each group took the effective count rate to be the average of the rates in its component cycles. We then performed a global fit on the resulting summed spectra. The  $^{37}\text{K}$  half-life extracted turned out to be insensitive to the number of cycles summed together for each spectrum. Figure 2 shows a simultaneous fit using the global-analysis method; it is of the same run for

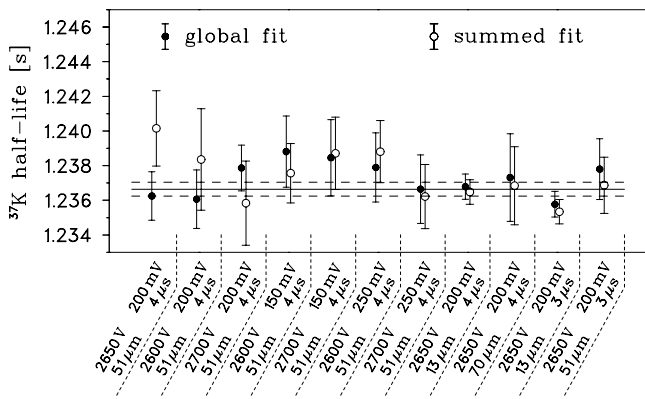


FIG. 3. The half-life obtained for  $^{37}\text{K}$  with different experimental conditions using the two analysis methods. The labels for each run are the detector bias, discriminator setting, degrader thickness and imposed deadtime. The solid line shows the best-fit half-life with the dashed lines representing the statistical uncertainty in the fit.

which the summed analysis is illustrated in Fig 1. The extracted values for the half-life obtained from the two analysis methods are well within uncertainties, as one can see from the results shown in Figs. 1 and 2.

### A. Systematic Uncertainties

The changing of parameters from run to run allowed us to test for potential systematic effects that could contribute to the uncertainty in the final results. In Fig. 3 we plot the half-life obtained for 11 different run conditions using both analysis techniques. Since two of the 13 runs had the same conditions as another run, each has been averaged with its twin and plotted as a single half-life. Each plotted result is labeled by the four measurement parameters that pertained to that result: detector bias, discriminator setting, degrader thickness and imposed deadtime. As already mentioned, each run produced two data streams, each with a different imposed deadtime. In all cases, the half-lives obtained from the two streams agreed very closely. Since both contain the same primary data, only the result from one of the data streams is presented in Fig. 3. No systematic dependence on measurement parameters is evident.

TABLE I. Half-life values for  $^{37}\text{K}$  obtained from two different analysis techniques. All of the uncertainties shown are purely statistical. The adopted half-life is taken to be the unweighted average of the two methods.

Method	half-life [s]
Summed analysis	1.23633(47)
Global analysis	1.23669(38)
Average $^{37}\text{K}$ half-life	1.23651(47)

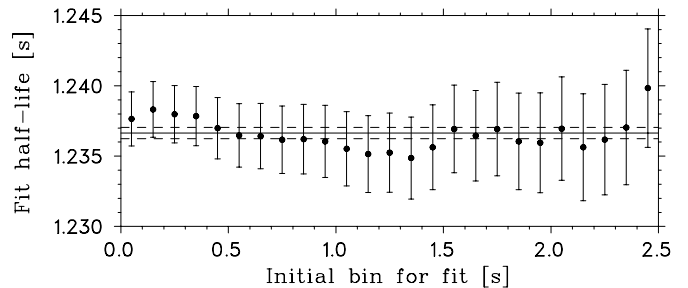


FIG. 4. Test for otherwise undetected short-lived impurities or for possible rate-dependent effects. Each point is the result of a separate fit to one of the runs as the starting time of the fitting range is increased. The solid and dashed lines correspond to the average half-life value and uncertainties given in Fig. 3.

In Table I we present the half-lives, averaged over all runs, obtained from the two different analysis techniques, “summed” and “global”. We take our final result to be the unweighted average of these two half-lives, with the statistical uncertainty on the average conservatively chosen to be the larger of the two individual values.

Although we regularly monitored impurities with the detector at the focal plane of MARS and accounted for the observed impurities in our fitting procedures, we nevertheless made an additional check at the analysis stage for unidentified short-lived impurities. We did this by artificially removing up to the first 3.0 s (60 channels) of the counting period in steps of 0.1 s. At each step the remaining channels in the reduced data set were fitted and a half-life extracted. The results are plotted in Fig. 4, from which it is clear from that the derived half-life is stable against these changes. This test also demonstrates our system’s independence of counting rate. We examined the sensitivity of our fit results to all the potential sources of systematic errors described above. The outcome is the error budget given in Table II. We found the greatest variation in the extracted lifetime when we fixed the value of the total impurity level to the amount observed in the MARS focal-plane detector rather than

TABLE II. Error budget for the  $^{37}\text{K}$  lifetime measurement. All of the values listed are in milliseconds.

Source	Uncertainty
Statistical	0.47
Systematics:	
Contaminants	0.72
Analysis method	0.30
Deadtime	0.20
Fitting range	0.13
Bias voltage	0.04
Discriminator threshold	0.04
Total systematic	0.82
Total uncertainty	0.94



leaving it free to vary in the fits. The next largest source of uncertainty was the counting statistics. Our final result for the half-life of  $^{37}\text{K}$  is:

$$1.23651(94) \text{ s.} \quad (4)$$

This 0.08% measurement is nearly an order of magnitude improvement over the previously accepted value [8] and now completely dominates the world average of the  $^{37}\text{K}$  half-life.

#### IV. $\mathcal{F}t$ -VALUE

We follow the convention used in Refs. [7] and [8] by defining the corrected  $\mathcal{F}t$  value for mirror nuclei which includes the variation due to the ratio of the Fermi to Gamow-Teller matrix elements. Specifically, the  $\mathcal{F}t_0$  value is defined as

$$\mathcal{F}t_0 = \mathcal{F}t C_V^2 |M_F^0|^2 \left[ 1 + \left( \frac{f_A}{f_V} \right) \rho^2 \right] \quad (5)$$

where experimentally  $\mathcal{F}t$  has already been defined in Eq. (1) in terms of the measured  $ft$  value and the small radiative and isospin-mixing corrections as calculated in Ref. [8]. The mixing ratio  $\rho$  defined by Eq. (3) is experimentally determined from a measurement of one of the angular correlations of the decay.

When calculating the  $\mathcal{F}t$  value, we take the branching ratio and total decay energy of  $^{37}\text{K}$  from the survey of Ref. [8]:  $\text{BR} = 97.99(14)\%$  and  $Q_{EC} = 6.14746(20) \text{ MeV}$ .

Using our new value for the half-life of  $^{37}\text{K}$ , we find

$$\mathcal{F}t = 4605.4 \pm 8.2 \text{ s.} \quad (6)$$

This result is four times more precise than the previous  $\mathcal{F}t$  value quoted in Ref. [7], and is now comparable to the precision of the three most precisely measured  $T = 1/2$  mirror nuclei. The branching ratio, no longer the half-life, is what now limits the precision of the  $\mathcal{F}t$  value. We have already made a new measurement of this branching ratio and are currently in the process of analyzing the data. This should reduce the uncertainty in the  $\mathcal{F}t$  value even further.

The only  $^{37}\text{K}$  correlation measurement published to date,  $B_\nu = -0.755(23)$  [9], can be used to determine a value for  $\rho$ . Using the recoil-order corrections of Holstein [18], we find  $\rho = -0.560_{-29}^{+24}$ , where the asymmetric error bars arise from the fact that the uncertainty in  $B_\nu$  is so large that the uncertainty on the extracted value of  $\rho$  is not Gaussian. Using this value of  $\rho$  and the  $\mathcal{F}t$  value above leads to

$$\mathcal{F}t_0 = 6057_{-122}^{+149} \text{ s.} \quad (7)$$

With our new lifetime measurement, the central value of  $\mathcal{F}t_0$  has changed and is now better aligned with other mirror transitions.

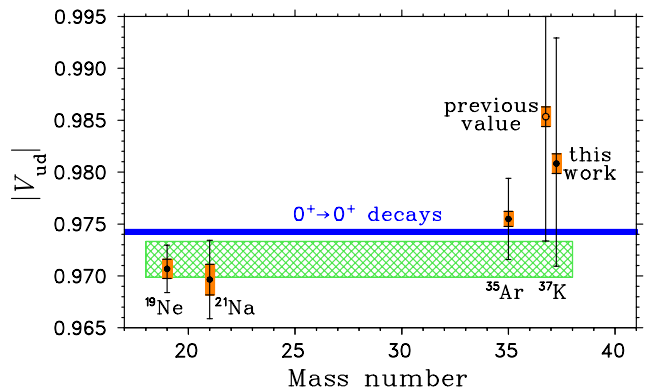


FIG. 5. (Colour online) Values of  $V_{ud}$  deduced for the four most precisely measured mirror transitions as a function of mass number. The smaller error bars with the filled in region represent the component of the total uncertainty arising from just  $\mathcal{F}t$  (the total error bars are all dominated by the correlation measurements). The hatched region represents the fit to the average ( $\chi^2/3 = 0.7$ ) yielding  $|V_{ud}| = 0.9718(17)$ . For comparison, the solid band shows the value of  $V_{ud}$  derived from the pure Fermi transitions.

Finally, noting that for a mixed transition,  $\mathcal{F}t_0$  is related to  $V_{ud}$  by [7]

$$V_{ud}^2 = \frac{K}{\mathcal{F}t_0 G_F^2 (1 + \Delta_V^R)}, \quad (8)$$

we calculate that from  $^{37}\text{K}$  alone

$$|V_{ud}| = 0.981_{-10}^{+12}. \quad (9)$$

This can be compared to the older value of 0.985(12). The uncertainty is barely affected by our improved half-life measurement because it is dominated by the large uncertainty in the  $B_\nu$  correlation parameter measurement.

In Fig. 5 we plot  $V_{ud}$  values for the four most precisely measured nuclear mirror transitions. The point for  $^{19}\text{Ne}$  has been updated from the survey of Ref. [8] to include recent lifetime results [19–21]. The figure shows that the main effect of the present  $^{37}\text{K}$  lifetime measurement is to shift its value of  $V_{ud}$  into better agreement with the other mirror nuclei and the  $0^+ \rightarrow 0^+$  transitions.

#### V. CONCLUSION

We have measured the half-life of  $^{37}\text{K}$ , the decay of which proceeds primarily via a mirror  $3/2^+ \rightarrow 3/2^+ \beta^+$  transition to its analog, the ground state in  $^{37}\text{Ar}$ . Our new result for the half-life is 1.23651(94) s. The 0.08% precision of this result is nearly an order of magnitude improvement over the previously accepted world average. The  $\mathcal{F}t$  value for the  $^{37}\text{K}$  mirror transition is now determined to 0.17% precision, and the corresponding values of  $\mathcal{F}t_0$  and  $V_{ud}$  have shifted into better alignment with values determined for the other well-measured mirror transitions. Nevertheless, the uncertainties of  $\mathcal{F}t_0$

and  $V_{ud}$  remain completely dominated by the correlation measurement for the transition. The results from improved correlation measurements, currently in progress by the TRINAT collaboration at TRIUMF [22], are required before the uncertainty on the mirror-transition value for  $V_{ud}$  can be improved.

## VI. ACKNOWLEDGEMENTS

We are grateful to the support staff of the Cyclotron Institute, especially Don May and George Kim for providing the primary beam. This work was supported by the U.S. Department of Energy under Grant No. DE-FG02-93ER40773 and Early Career Award ER41747, as well as the Robert A. Welch Foundation under Grant No. A-1397.

- 
- [1] J. C. Hardy and I. S. Towner, Phys. Rev. Lett. **94**, 092502 (Mar 2005)
- [2] J. C. Hardy and I. S. Towner, Phys. Rev. C **71**, 055501 (May 2005)
- [3] J. C. Hardy and I. S. Towner, Phys. Rev. C **79**, 055502 (2009)
- [4] M. Mendenhall *et al.* (UCNA Collaboration), Phys. Rev. C **87**, 032501 (Mar 2013), <http://link.aps.org/doi/10.1103/PhysRevC.87.032501>
- [5] B. Plaster *et al.* (UCNA Collaboration), Phys. Rev. C **86**, 055501 (Nov 2012), <http://link.aps.org/doi/10.1103/PhysRevC.86.055501>
- [6] D. Mund *et al.*, Phys. Rev. Lett. **110**, 172502 (Apr 2013), <http://link.aps.org/doi/10.1103/PhysRevLett.110.172502>
- [7] O. Naviliat-Cuncic and N. Severijns, Phys. Rev. Lett. **102**, 142302 (Apr 2009)
- [8] N. Severijns, M. Tandeci, T. Phalet, and I. S. Towner, Phys. Rev. C **78**, 055501 (Nov 2008)
- [9] D. Melconian *et al.*, Phys. Lett. B **649**, 370 (2007), ISSN 0370-2693
- [10] F. Schweizer, Phys. Rev. **110**, 1414 (Jun 1958)
- [11] R. W. Kavanagh and D. R. Goosman, Phys. Lett.. **12**, 229 (1964), ISSN 0031-9163, erratum Phys. Lett. **13**, 358 (1964)
- [12] G. Azuelos, J. E. Kitching, and K. Ramavataram, Phys. Rev. C **15**, 1847 (May 1977)
- [13] R. Tribble, C. Gagliardi, and W. Liu, Nucl. Instrum. Methods Phys. Res. B **56-57**, 956 (1991)
- [14] R. Tribble *et al.*, Nucl. Phys. A **701**, 278 (2002), ISSN 0375-9474, <http://www.sciencedirect.com/science/article/pii/S037594740200029>
- [15] V. Koslowsky *et al.*, Nucl. Instrum. Methods Phys. Res. A **401**, 289 (1997), ISSN 0168-9002, <http://www.sciencedirect.com/science/article/pii/S016890029700029>
- [16] V. Iacob *et al.*, Phys. Rev. C **74**, 055502 (Nov 2006), <http://link.aps.org/doi/10.1103/PhysRevC.74.055502>
- [17] V. Iacob *et al.*, Phys. Rev. C **82**, 035502 (Sep 2010), <http://link.aps.org/doi/10.1103/PhysRevC.82.035502>
- [18] B. Holstein, Rev. Mod. Phys. **46**, 789 (1974)
- [19] S. Triambak *et al.*, Phys. Rev. Lett. **109**, 042301 (Jul 2012), <http://link.aps.org/doi/10.1103/PhysRevLett.109.042301>
- [20] P. Ujjc *et al.*, Phys. Rev. Lett. **110**, 032501 (Jan 2013), <http://link.aps.org/doi/10.1103/PhysRevLett.110.032501>
- [21] L. J. Broussard *et al.*, Phys. Rev. Lett. **112**, 212301 (May 2014), <http://link.aps.org/doi/10.1103/PhysRevLett.112.212301>
- [22] D. Melconian *et al.* (2014), submitted to Proceedings of Science for the X Latin American Symposium on Nuclear Physics and Applications (X LASNPA).